

Antiferromagnetic Order and Magnetic Frustration in the Honeycomb Heavy-Fermion System $\text{Ce}(\text{Pt}_{1-x}\text{Pd}_x)_6\text{Al}_3$: ^{27}Al and ^{195}Pt NMR Studies

Shunsaku Kitagawa^{1,*}, Fumiya Hori^{1,†}, Kenji Ishida¹, Ryohei Oishi^{2,‡}, Yasuyuki Shimura², Takahiro Onimaru², and Toshiro Takabatake²

¹*Department of Physics, Graduate School of Science, Kyoto University, Kyoto 606-8502, Japan*

²*Department of Quantum Matter, Graduate School of Advanced Science and Engineering, Hiroshima University, Higashi-Hiroshima 739-8530, Japan*

Heavy-fermion systems with magnetic frustration offer a rich platform for investigating the interplay among Kondo screening, magnetic frustration, and quantum criticality. We report comprehensive ^{27}Al and ^{195}Pt nuclear magnetic resonance measurements on polycrystalline $\text{Ce}(\text{Pt}_{1-x}\text{Pd}_x)_6\text{Al}_3$ ($x = 0, 0.1, 0.2$, and 0.3). For $x = 0$, the Knight shift, linewidth, and nuclear spin-lattice relaxation rate reveal a paramagnetic heavy-fermion ground state persisting down to 0.1 K, characterized by a coherence temperature $T_{\text{coh}} \simeq 15$ K. Substituting Pd induces antiferromagnetic order at $T_N \simeq 3.5$ K, while suppressing T_{coh} . Comparison between $x = 0.1$ and $x = 0.3$ reveals a crossover from itinerant spin-density-wave antiferromagnetism to more localized-moment antiferromagnetism, indicating a shift toward the localized side of the Doniach phase diagram. These findings establish $\text{Ce}(\text{Pt}_{1-x}\text{Pd}_x)_6\text{Al}_3$ as a tunable platform to explore the competition between Kondo screening and magnetic frustration.

1. Introduction

Quantum materials in which several competing interactions coexist offer rich grounds for exploring non-trivial emergent phenomena such as quantum criticality and quantum spin-liquid (QSL) states.^{1–3} One canonical route to such competition arises when nearest-neighbor (J_1) and next-nearest-neighbor (J_2) exchange interactions are comparable in magnitude, leading to magnetic frustration. In insulating magnets, the realization of QSL states due to magnetic frustration has been actively studied in triangular, kagomé, zigzag or honeycomb networks.^{4–19} Recent theoretical and experimental studies have demonstrated that considering anisotropic magnetic interactions can lead to the emergence of novel low-energy excitations, such as Majorana fermions and nematic quasiparticles.^{20–31}

While many investigations focus on localized spins without conduction electrons, the interplay between localized f -electrons and conduction carriers in metallic systems represents an equally fascinating frontier.^{32,33} In f -electron compounds, theoretical studies have predicted that tuning the ratio of the Kondo coupling J_{cf} to the intersite magnetic interactions J_1 and J_2 can yield a wide variety of ground states, ranging from heavy Fermi liquids to magnetically ordered phases and possibly metallic QSLs.^{34–36} Moreover, it is well established that many heavy-fermion compounds exhibit unconventional superconductivity in the vicinity of a magnetic quantum critical point (QCP).^{37–42} In recent years, increasing attention has been drawn to superconductors on frustrated systems, such as kagomé networks, in which

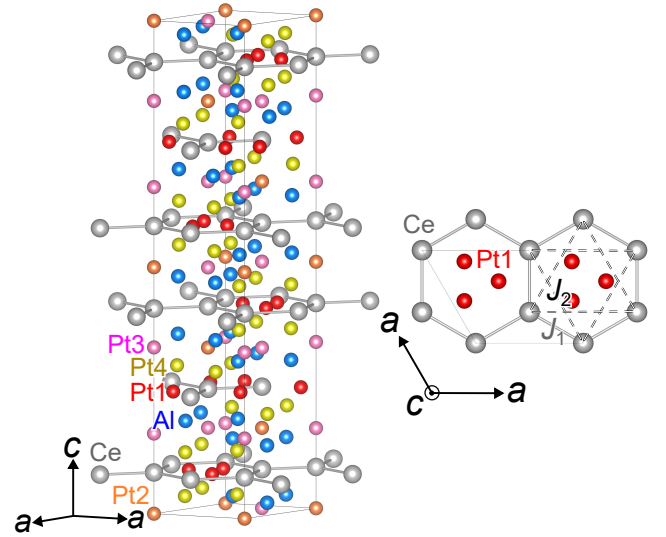


Fig. 1. (Color online) Crystal structure of CePt_6Al_3 drawn by VESTA.⁵⁰ A box indicates the unit cell. Ce atoms form a two-dimensional honeycomb network. There are four inequivalent Pt sites, whereas Al occupies a single crystallographic site. We represent nearest-neighbor interaction J_1 and next-nearest-neighbor interaction J_2 in the right panel.

unconventional pairing and ordered states have been reported.^{43–49} From this perspective, systems that host both strong Kondo interactions and magnetic frustration offer a unique platform to explore novel quantum phases.

$\text{Ce}(\text{Pt}_{1-x}\text{Pd}_x)_6\text{Al}_3$ is one of these candidate systems. CePt_6Al_3 crystallizes in the NdPt_6Al_3 -type trigonal structure with a centrosymmetric space group $R\bar{3}c$ (D_{3d}^6 , No. 167), in which Ce atoms form a two-dimensional honeycomb network (Fig. 1).⁵¹ This honeycomb arrangement naturally leads to magnetic frustration among the localized $4f$ moments due to the competing interactions

*E-mail address: kitagawa.shunsaku.8u@kyoto-u.ac.jp

†Present address: Department of Physics, Tohoku University, Sendai 980-8578, Japan

‡Present address: Research Institute for Electronic Science, Hokkaido University, Sapporo 001-0020, Japan

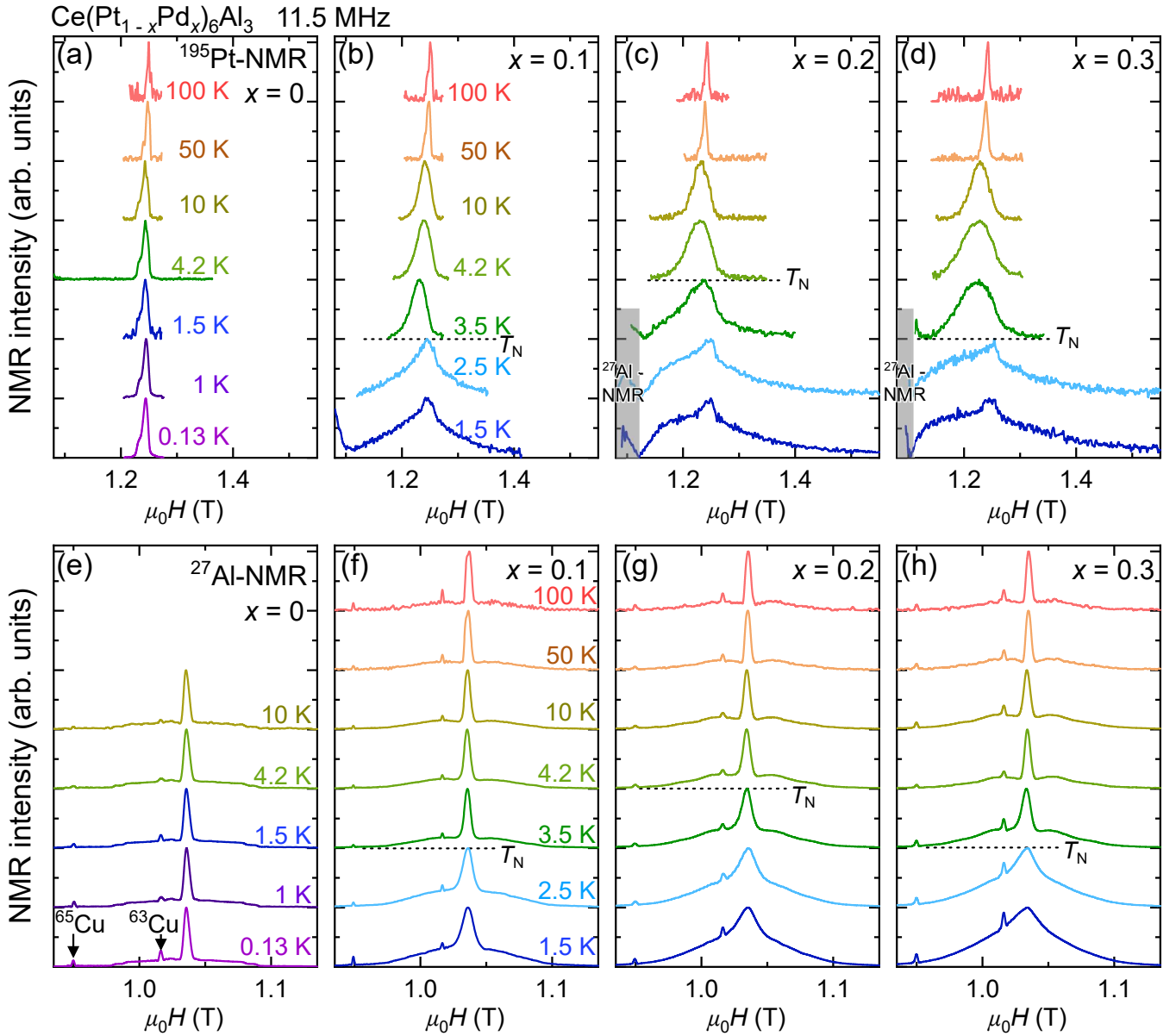


Fig. 2. (Color online) Temperature variation of the NMR spectra for $\text{Ce}(\text{Pt}_{1-x}\text{Pd}_x)_6\text{Al}_3$ measured at 11.5 MHz. (a)–(d): ^{195}Pt NMR spectra for $x = 0, 0.1, 0.2$, and 0.3 , respectively. (e)–(h): ^{27}Al NMR spectra for $x = 0, 0.1, 0.2$, and 0.3 , respectively.

between J_1 and J_2 . In related compounds where Ce is replaced by other rare-earth elements, a variety of magnetic structures have been observed.^{52–54} The measurements of specific heat, magnetic susceptibility, and electrical resistivity on CePt_6Al_3 indicate the formation of a heavy-electron state below Kondo temperature $T_K \sim 10$ K, suggesting a strong competition between Kondo screening and frustrated magnetic interactions.⁵⁵

Partial substitution of Pt by Pd in CePt_6Al_3 retains the trivalent state of Ce, while systematically reducing the absolute value of the paramagnetic Curie temperature θ_p .^{56,57} At substitution levels $x \geq 0.1$, a long-range antiferromagnetic (AFM) order emerges, implying that Pd doping reduces Kondo coupling J_{cf} or/and relieves magnetic frustration. Specific heat measurements reveal that the entropy recovered just above the Néel temperature T_N increases with x and that the estimated T_K decreases from ~ 10 K at $x = 0$ to ~ 3.5 K at $x = 0.3$.

These results suggest a gradual suppression of the Kondo effect with Pd substitution.⁵⁶

Furthermore, the frustration parameter $f = |\theta_p|/T_N$ decreases with increasing x , although care must be taken because both θ_p and T_N can be influenced by the Kondo effect. The sign of resistivity change below T_N indicates a difference in the nature of the antiferromagnetism: At $x = 0.1$, a spin-density-wave (SDW)-like AFM order is realized, whereas at $x \geq 0.2$, the behavior is more consistent with a localized-moment type of AFM order.⁵⁶

In this work, to microscopically investigate how the magnetic properties evolve with Pd substitution, we performed ^{27}Al and ^{195}Pt nuclear magnetic resonance (NMR) measurements on polycrystalline $\text{Ce}(\text{Pt}_{1-x}\text{Pd}_x)_6\text{Al}_3$ for $x = 0, 0.1, 0.2$, and 0.3 . Our results indicate that CePt_6Al_3 remains paramagnetic down to 0.1 K, while Pd substitution induces AFM order. By comparing the results at $x = 0.1$ with those at $x = 0.3$,

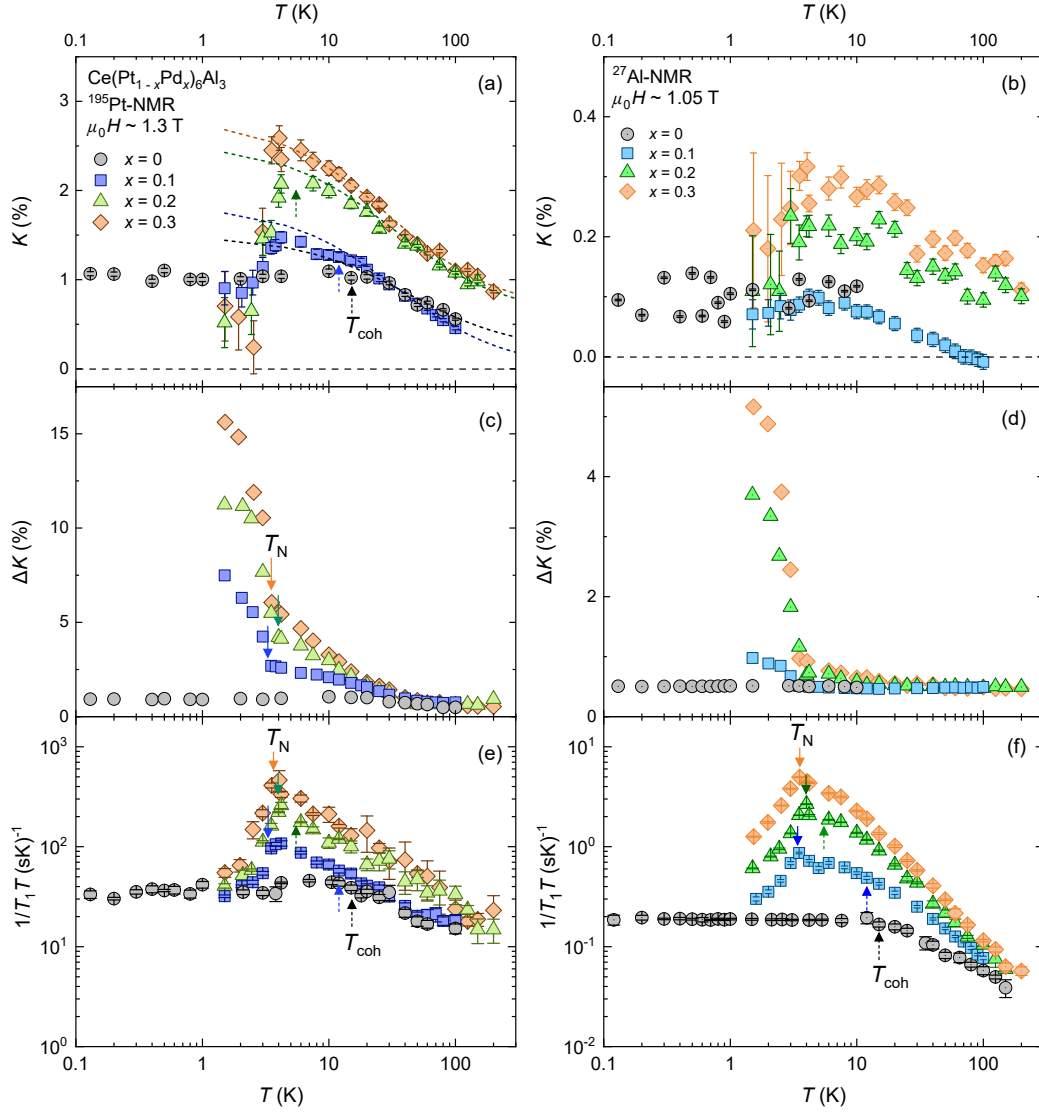


Fig. 3. (Color online) Temperature dependence of the NMR quantities for $\text{Ce}(\text{Pt}_{1-x}\text{Pd}_x)_6\text{Al}_3$. (a), (b): Knight shift K for (a) ^{195}Pt and (b) ^{27}Al . The broken curves indicate Curie-Weiss behavior. (c), (d): Linewidth ΔK for (c) ^{195}Pt and (d) ^{27}Al . (e), (f): Nuclear spin-lattice relaxation rate $1/T_1 T$ for (e) ^{195}Pt and (f) ^{27}Al . The suppression of $1/T_1 T$ and the saturation of K at low temperatures signal the formation of heavy-fermion coherence, whereas the anomalies at T_N indicate the onset of antiferromagnetic order. The solid (dashed) arrows indicate T_N (T_{coh}).

we identify a crossover from itinerant to localized magnetism as the Kondo coupling is suppressed, which is consistent with the bulk measurements.^{56,57} These findings demonstrate that the competition between Kondo screening and magnetic frustration governs the evolution of the ground state in $\text{Ce}(\text{Pt}_{1-x}\text{Pd}_x)_6\text{Al}_3$, providing a unique platform to explore quantum criticality.

2. Experimental

Polycrystalline samples of $\text{Ce}(\text{Pt}_{1-x}\text{Pd}_x)_6\text{Al}_3$ with $x = 0, 0.1, 0.2$, and 0.3 were synthesized by a conventional arc-melting method followed by annealing.⁵⁶ The Pd composition x determined by wavelength-dispersive electron-probe microanalysis for the main phase did not deviate from the nominal value x within the resolution. ^{27}Al (nuclear spin $I = 5/2$, gyromagnetic ratio $^{27}\gamma/2\pi = 11.094$ MHz/T, nuclear quadrupole moment $^{27}Q = 0.1466 \times 10^{-28}$ m²) and ^{195}Pt ($I = 1/2$, $^{195}\gamma/2\pi =$

9.153 MHz/T) NMR measurements were carried out using a conventional spin-echo technique.^{58,59} The magnetic field-sweep NMR spectra were obtained by recording the spin-echo signal observed after a standard $\pi/2-\pi$ radio frequency pulse sequence at 11.5 MHz. The magnetic field was calibrated using a $^{63/65}\text{Cu}$ [$^{63(65)}\gamma/2\pi = 11.285(12.089)$ MHz/T]-NMR signal with the Knight shift $K_{\text{Cu}} = 0.2385\%$ from a NMR coil.⁶⁰ Knight shift was determined from the peak position of the NMR spectrum, and the full width at half-maximum (FWHM), ΔK , was used to characterize the spectral linewidth. The nuclear spin-lattice relaxation rate $1/T_1$ was measured at the central peak of the NMR spectra. $1/T_1$ was evaluated by fitting the relaxation curve of the nuclear magnetization after saturation to a theoretical function for the nuclear spin $I = 1/2$ (^{195}Pt), which is a single exponential function, and that for $I = 5/2$ (^{27}Al). Temperature control down to 0.1 K was achieved using a $^3\text{He}-^4\text{He}$ dilution

refrigerator.

3. Results and Discussion

3.1 Static magnetic properties

Figure 2 presents the ^{195}Pt - and ^{27}Al -NMR spectra for $\text{Ce}(\text{Pt}_{1-x}\text{Pd}_x)_6\text{Al}_3$ with $x = 0, 0.1, 0.2$, and 0.3 over a wide temperature range. The ^{27}Al NMR spectra are relatively sharp and exhibit well-resolved satellite peaks, reflecting the existence of electric field gradients. In contrast, the ^{195}Pt NMR spectra are considerably broader and complex shapes even in the paramagnetic state, which can be attributed to the presence of four crystallographically inequivalent Pt sites, as shown in Fig. 1. The line widths of the ^{27}Al and ^{195}Pt spectra are almost unchanged with increasing Pd concentration. Upon cooling, the linewidth of ^{195}Pt grows more markedly than that of ^{27}Al , indicating a larger hyperfine coupling constant for Pt and the presence of significant magnetic anisotropy. The difference in the hyperfine coupling constants may originate from the distances from the Ce atoms, as shown in Fig. 1.

For $x \geq 0.1$, a pronounced broadening of the spectra is observed below approximately 3.5 K, signaling the onset of long-range AFM order. In contrast, no discernible broadening is detected for $x = 0$ down to 0.1 K, indicating the absence of magnetic order. In the ordered state, the ^{27}Al NMR spectra broaden symmetrically, whereas the ^{195}Pt spectra exhibit an asymmetric broadening. This asymmetry likely originates from the different magnitudes and directions of internal magnetic fields at the four distinct Pt sites. However, because the present measurements were performed on powdered samples, detailed information about the magnetic structure could not be determined.

The temperature dependence of the Knight shift K , determined from the peak position of the NMR spectrum, is summarized in Figs. 3(a) and 3(b). At high temperatures, ^{195}K for all compositions follows a Curie–Weiss behavior, which reflects the dominance of localized moment contributions. On cooling, ^{195}K levels off below the coherence temperature T_{coh} , indicating the formation of a coherent heavy-fermion state. Here, T_{coh} is defined as the characteristic temperature below which the ^{195}K Knight shift begins to deviate from Curie–Weiss behavior. For $x = 0$, T_{coh} is estimated to be approximately 15 K, whereas it decreases to ~ 12.5 K for $x = 0.1$. Although no distinct anomaly is observed at $x = 0.2$, there is a subtle deviation near T_K estimated from the magnetic entropy (~ 4.5 K). The suppression of the Kondo effect with Pd substitution is consistent with the previous measurements.⁵⁶⁾ Note that, as discussed later, an anomaly at around T_{coh} is also observed in $1/T_1T$, particularly for ^{27}Al , although the anomaly in ^{195}K at T_{coh} is not pronounced.

The Knight shift is proportional to the bulk magnetic susceptibility χ through the hyperfine interaction, as expressed by the relation,

$$K = \frac{A_{\text{hf}}}{N_A \mu_B} \chi + K_0, \quad (1)$$

where A_{hf} is the hyperfine coupling constant, N_A is the

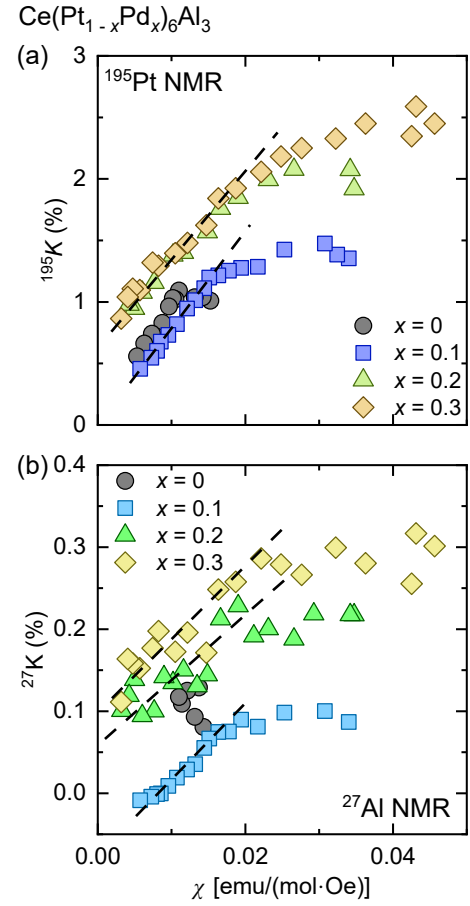


Fig. 4. (Color online) K - χ plot for (a) ^{195}Pt - and (b) ^{27}Al -NMR in $\text{Ce}(\text{Pt}_{1-x}\text{Pd}_x)_6\text{Al}_3$. The magnetic susceptibility data were obtained from Ref. 56. The broken lines indicate the guide for the eyes.

Avogadro constant, μ_B is the Bohr magneton, and K_0 is the temperature-independent component of the Knight shift. The value of A_{hf} can be determined from the slope of the K - χ plot shown in Figs. 4(a) and 4(b). For all values of x , a change in slope is observed around $\chi \sim 0.02$ [emu/(mol·Oe)]. This is because, at low temperatures, the magnetic susceptibility is affected by magnetic impurities,⁵⁶⁾ whereas the Knight shift selectively probes the intrinsic electronic properties in the sample. Therefore, A_{hf} was determined by fitting a linear relation in the high-temperature region, where both K and χ are small. The estimated A_{hf} and K_0 are summarized in Table I. Note that, as the present measurements were performed on polycrystalline samples, the estimated A_{hf} reflects the average values. As shown in Table I, A_{hf} at the Pt site is approximately 9 times larger than that at the Al site.

Figures 3(c) and 3(d) show the temperature dependence of FWHM of the NMR spectrum, ΔK . For $x \geq 0.1$, a sharp increase in ΔK is observed below $T_N \simeq 3.5$ K, consistent with the development of static staggered internal fields associated with AFM order. In contrast, for $x = 0$, no such anomaly in ΔK is detected down to 0.1 K, reinforcing the absence of magnetic order. As mentioned above, the larger sensitivity of the ^{195}Pt linewidth com-

Table I. Hyperfine coupling constant A_{hf} (in T/ μ_B) and temperature-independent Knight shift K_0 (in %) in $\text{Ce}(\text{Pt}_{1-x}\text{Pd}_x)_6\text{Al}_3$

x	Nucleus	T (K)	A_{hf} (T/ μ_B)	K_0 (%)
0.0	^{195}Pt	≥ 10	0.52 ± 0.04	0.04 ± 0.06
0.1	^{195}Pt	≥ 18	0.44 ± 0.01	-0.02 ± 0.05
	^{27}Al	≥ 18	0.044 ± 0.01	-0.064 ± 0.007
0.2	^{195}Pt	≥ 15	0.34 ± 0.01	0.69 ± 0.03
	^{27}Al	≥ 15	0.038 ± 0.008	0.07 ± 0.02
0.3	^{195}Pt	≥ 15	0.34 ± 0.02	0.78 ± 0.03
	^{27}Al	≥ 15	0.041 ± 0.006	0.11 ± 0.01

pared to that of ^{27}Al can be attributed to the larger hyperfine coupling constants at the Pt sites. These observations collectively confirm that Pd substitution induces AFM order and simultaneously suppresses T_{coh} in $\text{Ce}(\text{Pt}_{1-x}\text{Pd}_x)_6\text{Al}_3$.

3.2 Dynamic magnetic properties

Figures 3(e) and 3(f) show the temperature dependence of $1/T_1T$ for $\text{Ce}(\text{Pt}_{1-x}\text{Pd}_x)_6\text{Al}_3$ with $x = 0, 0.1, 0.2$, and 0.3 . $1/T_1T$ exhibits a systematic variation with x and appears to show little dependence on the applied magnetic field, in contrast to the NMR spectrum. At temperatures above 100 K, $1/T_1T$ of ^{195}Pt is nearly temperature independent for all samples, indicating a dominant contribution from conduction electrons rather than localized $4f$ moments. With decreasing temperature, $1/T_1T$ increases approximately following a $1/T$ behavior, consistent with the development of magnetic fluctuations associated with localized moments. Below T_{coh} , $1/T_1T$ either saturates (for $x = 0$) or shows a change in slope (for $x = 0.1$ and 0.2), reflecting the crossover to a heavy-fermion state,⁶¹ similar to the Knight shift.

For samples with $x \geq 0.1$, a divergence of $1/T_1T$ is observed upon approaching $T_N \simeq 3.5$ K, signaling critical slowing down of magnetic fluctuations. Below T_N , $1/T_1T$ drops sharply, indicating the opening of a gap in the magnetic excitation spectrum due to the establishment of AFM order. The magnitude of $1/T_1T$ at the ^{195}Pt sites is about two orders of magnitude larger than that at the ^{27}Al sites, which can also be attributed to the stronger hyperfine coupling constant at the Pt sites. These results are fully consistent with the Knight shift and linewidth analyses and further support the scenario that Pd substitution induces a transition from a paramagnetic heavy-fermion state to an antiferromagnetically ordered state in $\text{Ce}(\text{Pt}_{1-x}\text{Pd}_x)_6\text{Al}_3$.

3.3 Compositional Phase Diagram

Figure 5 summarizes the Pd concentration dependence of T_{coh} and T_N determined from the NMR measurements. T_{coh} decreases monotonically from approximately 15 K at $x = 0$ and becomes undetectable at $x = 0.3$, reflecting a systematic suppression of the Kondo coupling J_{cf} with increasing Pd content. In contrast, T_N remains nearly constant at around 3.5 K for $0.1 \leq x \leq 0.3$, while it

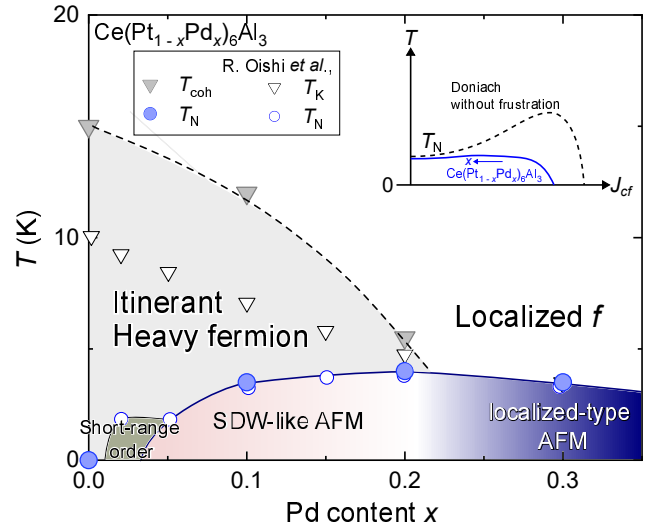


Fig. 5. (Color online) Pd concentration dependence of the Néel temperature T_N and the coherence temperature T_{coh} determined from the NMR measurements. T_N and Kondo temperature T_K determined from the magnetic susceptibility and specific heat measurements are also shown.⁵⁶⁾ (Inset) Schematic image of the magnetic phase diagram of $\text{Ce}(\text{Pt}_{1-x}\text{Pd}_x)_6\text{Al}_3$ compared with the conventional Doniach phase diagram.

abruptly vanishes with decreasing x from 0.1 to 0, suggesting the existence of a QCP near $x_c \simeq 0$. Short-range magnetic order was reported at $x = 0.025$ in magnetic susceptibility measurements.⁵⁶⁾

The contrasting trends between T_{coh} and T_N suggest that, in addition to the reduction of J_{cf} , other factors such as magnetic frustration may play a significant role in stabilizing the AFM order. Within the conventional Doniach framework,⁶²⁾ decreasing J_{cf} is expected to first enhance and then suppress T_N as the system moves away from the QCP. As a result, T_N of prototypical heavy-fermion systems such as $\text{CeCu}_{6-x}\text{Au}_x$ ⁶³⁾ and CeNiGe_3 under pressure⁶⁴⁾ exhibits a clear dome-shaped dependence on control parameters. In contrast, T_N in $\text{Ce}(\text{Pt}_{1-x}\text{Pd}_x)_6\text{Al}_3$ remains nearly constant for $x \geq 0.1$. One possible scenario that explains this unconventional change in $T_N(x)$ is that in $x = 0$, the system lies in a region where long-range AFM order would be expected without frustration. However, strong competing interactions among Ce moments suppress the ordering temperature to zero, effectively stabilizing a QCP. As Pd is substituted, J_{cf} decreases, which would typically reduce T_N ; at the same time, the Pd substitution may relieve magnetic frustration. In this regime, the opposing effects of reduced J_{cf} (suppressing T_N) and weakened frustration (enhancing T_N) may effectively compensate for each other, leading to an almost constant T_N for $x \geq 0.1$, as shown in the inset of Fig. 5. This scenario is consistent with the systematic decrease in the frustration parameter $f = |\theta_p|/T_N$ as a function of x observed in the previous measurements.⁵⁶⁾ The weakening of magnetic frustration with increasing Pd content may originate from a reduction in the competition between J_1 and J_2 interactions. In addition, an enhancement of interlayer coupling, suggested by the decrease in the c -axis length with Pd sub-

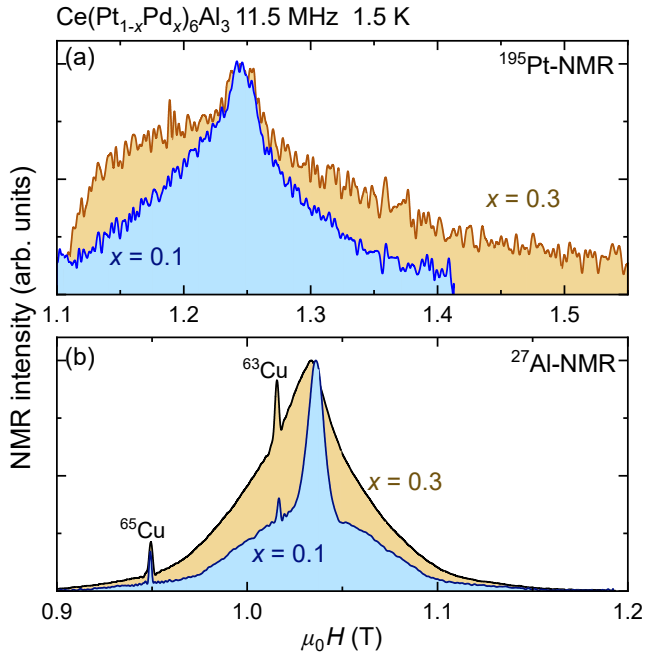


Fig. 6. (Color online) Comparison of (a) ^{195}Pt -NMR and (b) ^{27}Al -NMR spectra at 1.5 K for $x = 0.1$ and $x = 0.3$ of $\text{Ce}(\text{Pt}_{1-x}\text{Pd}_x)_6\text{Al}_3$.

stitution,⁵⁶⁾ reduces the two-dimensionality of the electronic state, which would also act to suppress magnetic frustration.

3.4 Nature of the Antiferromagnetic Order

Comparison between the results at $x = 0.1$ and those at $x = 0.2$ and 0.3 reveals a notable change in the character of the AFM order. For $x = 0.1$, the presence of a residual heavy-fermion coherence just above T_N , as indicated by the saturation of the Knight shift and $1/T_1T$, suggests an itinerant SDW-type AFM order. In this regime, the ordered moments are expected to be relatively small, and Fermi surface instabilities predominantly drive the magnetism. In contrast, for $x = 0.3$, no clear signature of heavy-fermion coherence is observed above T_N . The Knight shift and $1/T_1T$ values are larger in the paramagnetic state compared to $x = 0.1$, indicating enhanced fluctuating local moments.

In addition, as shown in Fig. 6, both the ^{27}Al and ^{195}Pt spectra for $x = 0.3$ broaden significantly compared to those for $x = 0.1$, suggesting an increase in the ordered moment. While structural features in the ^{195}Pt spectra are also observed, because of the powder-sample measurements and the presence of multiple crystallographically distinct Pt sites, it is difficult to make definitive conclusions regarding changes in magnetic structure. These observations suggest that the antiferromagnetism in the $x = 0.3$ sample is more localized, with larger ordered moment associated with the $4f$ electrons. Thus, Pd substitution drives the system from an itinerant SDW regime at $x = 0.1$ toward a localized moment AFM regime for $x = 0.3$. This evolution is consistent with a movement toward the localized side of the Doniach phase diagram as the Kondo coupling J_{cf} becomes weaker. Our findings

provide microscopic evidence that chemical substitution in $\text{Ce}(\text{Pt}_{1-x}\text{Pd}_x)_6\text{Al}_3$ enables controlled tuning between itinerant and localized magnetism.

3.5 Prospects for Unconventional Superconductivity

Although superconductivity has not yet been observed in $\text{Ce}(\text{Pt}_{1-x}\text{Pd}_x)_6\text{Al}_3$, the proximity to a magnetic QCP near $x_c \simeq 0$ raises the intriguing possibility of its emergence. Unconventional superconductivity often appears in the vicinity of a magnetic QCP, where magnetic fluctuations can mediate unconventional pairing mechanisms.^{40,65–67)} Given the evidence for a QCP and the suppression of the Kondo scale with Pd substitution, $\text{Ce}(\text{Pt}_{1-x}\text{Pd}_x)_6\text{Al}_3$ represents a promising candidate for the realization of such superconductivity. Furthermore, the presence of competing interactions in the honeycomb network of Ce ions could enrich the pairing landscape, potentially leading to novel superconducting states that intertwine with magnetic frustration.^{68–70)} To explore this possibility, future studies with finer control of the Pd concentration near x_c , higher sample purity, and application of external pressure would be highly desirable. Moreover, the combination of frustration and quantum criticality in $\text{Ce}(\text{Pt}_{1-x}\text{Pd}_x)_6\text{Al}_3$ offers a rare opportunity to investigate the largely unexplored relationship between magnetic frustration and unconventional superconductivity in correlated electron systems.

4. Conclusion

We have performed comprehensive ^{27}Al and ^{195}Pt nuclear magnetic resonance measurements on polycrystalline $\text{Ce}(\text{Pt}_{1-x}\text{Pd}_x)_6\text{Al}_3$ with $x = 0, 0.1, 0.2$, and 0.3 to investigate the evolution of magnetic properties as a function of Pd substitution. The Knight shift, linewidth, and nuclear spin-lattice relaxation rate collectively reveal that CePt_6Al_3 remains a paramagnetic heavy-fermion metal down to 0.1 K, characterized by $T_{\text{coh}} \simeq 15$ K. In contrast, Pd substitution at $x \geq 0.1$ induces long-range AFM order below $T_N \simeq 3.5$ K, accompanied by a suppression of T_{coh} . The distinct behaviors of T_{coh} and T_N imply that Pd doping not only reduces the Kondo coupling J_{cf} but also partially relieves the underlying magnetic frustration. A QCP is suggested to exist near $x_c \simeq 0$. Comparison between $x = 0.1$ and $x = 0.3$ reveals a crossover from itinerant SDW-type to localized moment antiferromagnetism as the Kondo effect weakens. These findings establish $\text{Ce}(\text{Pt}_{1-x}\text{Pd}_x)_6\text{Al}_3$ as a unique platform where the interplay between Kondo screening and magnetic frustration can be systematically tuned by chemical substitution. The combination of magnetic frustration and quantum criticality provides an exciting opportunity to explore the potential emergence of unconventional superconductivity and exotic quantum phases in this system.

acknowledgments

This work was supported by Grants-in-Aid for Scientific Research (KAKENHI Grant No. JP20KK0061, No. JP20H00130, No. JP21K03473, No. JP21K18600, No. JP22H04933, No. JP22H01168, No. JP22KJ2336, No. JP23H01124, No. JP23K22439 and No. JP23K25821)

from the Japan Society for the Promotion of Science, by JST SPRING(Grant No. JPMJSP2110) from the Japan Science and Technology Agency, by research support funding from the Kyoto University Foundation, by ISHIZUE 2024 of Kyoto University Research Development Program, by Murata Science and Education Foundation, and by the JGC-S Scholarship Foundation. Liquid helium is supplied by the Low Temperature and Materials Sciences Division, Agency for Health, Safety and Environment, Kyoto University.

- 1) P. W. Anderson, *Materials Research Bulletin* **8**, 153 (1973).
- 2) L. Balents, *Nature* **464**, 199 (2010).
- 3) Y. Zhou, K. Kanoda, and T.-K. Ng, *Rev. Mod. Phys.* **89**, 025003 (2017).
- 4) X. Obradors, A. Labarta, A. Isalgue, J. Tejada, J. Rodriguez, and M. Pernet, *Solid State Commun.* **65**, 189 (1988).
- 5) Y. Shimizu, K. Miyagawa, K. Kanoda, M. Maesato, and G. Saito, *Phys. Rev. Lett.* **91**, 107001 (2003).
- 6) S. Nakatsuji, Y. Nambu, H. Tonomura, O. Sakai, S. Jonas, C. Broholm, H. Tsunetsugu, Y. Qiu, and Y. Maeno, *Science* **309**, 1697 (2005).
- 7) Y. Okamoto, M. Nohara, H. Aruga-Katori, and H. Takagi, *Phys. Rev. Lett.* **99**, 137207 (2007).
- 8) O. Smirnova, M. Azuma, N. Kumada, Y. Kusano, M. Matsuda, Y. Shimakawa, T. Takei, Y. Yonesaki, and N. Kinomura, *J. Am. Chem. Soc.* **131**, 8313 (2009).
- 9) K. A. Ross, L. Savary, B. D. Gaulin, and L. Balents, *Phys. Rev. X* **1**, 021002 (2011).
- 10) S. Yan, D. A. Huse, and S. R. White, *Science* **332**, 1173 (2011).
- 11) T.-H. Han, J. S. Helton, S. Chu, D. G. Nocera, J. A. Rodriguez-Rivera, C. Broholm, and Y. S. Lee, *Nature* **492**, 406 (2012).
- 12) S. Kitagawa, T. Sekiya, S. Araki, T. C. Kobayashi, K. Ishida, T. Kambe, T. Kimura, N. Nishimoto, K. Kudo, and M. Nohara, *J. Phys. Soc. Jpn.* **84**, 093701 (2015).
- 13) M. Fu, T. Imai, T.-H. Han, and Y. S. Lee, *Science* **350**, 655 (2015).
- 14) Y. Kawasaki, S. Yamazaki, A. Pustogow, and N. Tajima, *J. Phys. Soc. Jpn.* **92**, 065001 (2023).
- 15) F. Iwase, *J. Phys. Soc. Jpn.* **92**, 074704 (2023).
- 16) K. Eto, Y. Okamoto, N. Katayama, H. Ishikawa, K. Kindo, and K. Takenaka, *J. Phys. Soc. Jpn.* **92**, 094707 (2023).
- 17) S. Kogure, M. Takeda, K. Morita, Y. Fukumoto, M. Saito, and H. Tanaka, *J. Phys. Soc. Jpn.* **92**, 113703 (2023).
- 18) K. Nihongi, T. Kida, D. Yamamoto, Y. Narumi, J. Zaccaro, Y. Kousaka, K. Inoue, Y. Uwatoko, K. Kindo, and M. Hagiwara, *J. Phys. Soc. Jpn.* **93**, 084704 (2024).
- 19) F. Hori, S. Kitagawa, K. Ishida, S. Mizutani, Y. Ohmagari, and T. Onimaru, *J. Phys. Soc. Jpn.* **93**, 114702 (2024).
- 20) A. Kitaev, *Ann. Phys.* **321**, 27111 (2006).
- 21) Y. Shen, Y.-D. Li, H. Wo, Y. Li, S. Shen, B. Pan, Q. Wang, H. C. Walker, P. Steffens, M. Boehm, Y. Hao, D. L. Quintero-Castro, L. W. Harriger, J. A. Rodriguez-Rivera, G. Chen, and J. Zhao, *Nature* **540**, 559 (2016).
- 22) A. Banerjee, J. Yan, J. Knolle, C. A. Bridges, M. B. Stone, M. D. Lumsden, D. G. Mandrus, D. A. Tennant, R. Moessner, and S. E. Nagler, *Science* **356**, 1055 (2017).
- 23) J. A. M. Paddison, M. Daum, Z. Dun, G. Ehlers, H. Zhou, and M. Mourigal, *Nat. Phys.* **13**, 117 (2017).
- 24) Y. Kasahara, T. Ohnishi, Y. Mizukami, O. Tanaka, S. Ma, K. Sugii, N. Kurita, H. Tanaka, J. Nasu, Y. Motome, and Y. Matsuda, *Nature* **559**, 227 (2018).
- 25) K. Kitagawa, T. Takayama, Y. Matsumoto, G. Jackeli, and H. Takagi, *Nature* **554**, 341 (2018).
- 26) F. Hori, K. Kinjo, S. Kitagawa, K. Ishida, S. Mizutani, R. Yamamoto, Y. Ohmagari, and T. Onimaru, *Commun. Mater.* **4**, 55 (2023).
- 27) S. Yoshimoto, Y. Tabata, T. Waki, and H. Nakamura, *J. Phys. Soc. Jpn.* **92**, 094705 (2023).
- 28) T. Yamada and S.-i. Suga, *J. Phys. Soc. Jpn.* **92**, 114705 (2023).
- 29) H. Saito and C. Hotta, *Phys. Rev. Lett.* **132**, 166701 (2024).
- 30) F. Sato, T. Aoyama, S. Kawaguchi, H. Gotou, Y. Imai, and K. Ohgushi, *J. Phys. Soc. Jpn.* **93**, 093601 (2024).
- 31) H. Saito, H. Nakai, and C. Hotta, *J. Phys. Soc. Jpn.* **93**, 034701 (2024).
- 32) C. L. Yang, S. Tsuda, K. Umeo, Y. Yamane, T. Onimaru, T. Takabatake, N. Kikugawa, T. Terashima, and S. Uji, *Phys. Rev. B* **96**, 045139 (2017).
- 33) R. Kuchler, C. Stingl, Y. Tokiwa, M. S. Kim, T. Takabatake, and P. Gegenwart, *Phys. Rev. B* **96**, 241110 (2017).
- 34) P. Coleman and A. H. Nevidomskyy, *J. Low Temp. Phys.* **161**, 1827202 (2010).
- 35) K. Guo, J. Ye, S. Guan, and S. Jia, *Phys. Rev. B* **107**, 205151 (2023).
- 36) Y. Tokiwa, J. J. Ishikawa, S. Nakatsuji, and P. Gegenwart, *Nat. Mater.* **13**, 3567359 (2014).
- 37) F. Steglich, J. Aarts, C. D. Bredl, W. Lieke, D. Meschede, W. Franz, and H. Schäfer, *Phys. Rev. Lett.* **43**, 1892 (1979).
- 38) H. R. Ott, H. Rudigier, Z. Fisk, and J. L. Smith, *Phys. Rev. Lett.* **50**, 1595 (1983).
- 39) G. R. Stewart, Z. Fisk, J. O. Willis, and J. L. Smith, *Phys. Rev. Lett.* **52**, 679 (1984).
- 40) C. Pfleiderer, *Rev. Mod. Phys.* **81**, 1551 (2009).
- 41) D. Aoki, J.-P. Brison, J. Flouquet, K. Ishida, G. Knebel, Y. Tokunaga, and Y. Yanase, *J. Phys.: Cond. Matt.* **34**, 243002 (2022).
- 42) S. Kitagawa, K. Nakanishi, H. Matsumura, Y. Takahashi, K. Ishida, Y. Tokunaga, H. Sakai, S. Kambe, A. Nakamura, Y. Shimizu, Y. Homma, D. Li, F. Honda, A. Miyake, and D. Aoki, *J. Phys. Soc. Jpn.* **93**, 123701 (2024).
- 43) D. Jerome, *Science* **252**, 1509 (1991).
- 44) K. Takada, H. Sakurai, E. Takayama-Muromachi, F. Izumi, R. A. Dilanian, and T. Sasaki, *Nature* **422**, 53 (2003).
- 45) S. Kitagawa, K. Ishida, T. C. Kobayashi, Y. Matsubayashi, D. Hirai, and Z. Hiroi, *J. Phys. Soc. Jpn.* **89**, 053701 (2020).
- 46) B. R. Ortiz, S. M. L. Teicher, Y. Hu, J. L. Zuo, P. M. Sarte, E. C. Schueller, A. M. M. Abeykoon, M. J. Krogstad, S. Rosenkranz, R. Osborn, R. Seshadri, L. Balents, J. He, and S. D. Wilson, *Phys. Rev. Lett.* **125**, 247002 (2020).
- 47) Z. Wang, Y.-X. Jiang, J.-X. Yin, Y. Li, G.-Y. Wang, H.-L. Huang, S. Shao, J. Liu, P. Zhu, N. Shumiya, M. S. Hossain, H. Liu, Y. Shi, J. Duan, X. Li, G. Chang, P. Dai, Z. Ye, G. Xu, Y. Wang, H. Zheng, J. Jia, M. Z. Hasan, and Y. Yao, *Phys. Rev. B* **104**, 075148 (2021).
- 48) Y. Xiang, Q. Li, Y. Li, W. Xie, H. Yang, Z. Wang, Y. Yao, and H.-H. Wen, *Nat. Commun.* **12**, 6727 (2021).
- 49) K. Fukushima, K. Obata, S. Yamane, Y. Hu, Y. Li, Y. Yao, Z. Wang, Y. Maeno, and S. Yonezawa, *Nat. Commun.* **15**, 2888 (2024).
- 50) K. Momma and F. Izumi, *J. Appl. Crystallogr.* **44**, 1272 (2011).
- 51) F. Eustermann, F. Stegemann, K. Renner, and O. Janka, *Z. Anorg. Allg. Chem.* **643**, 183671843 (2017).
- 52) R. Oishi, Y. Shimura, K. Umeo, T. Onimaru, and T. Takabatake, *J. Phys. Soc. Jpn.* **91**, 124706 (2022).
- 53) R. Oishi, C. Ritter, M. M. Kozá, D. T. Adroja, T. Onimaru, Y. Shimura, K. Umeo, and T. Takabatake, *Phys. Rev. B* **110**, 144411 (2024).
- 54) R. Oishi, Y. Shimura, K. Umeo, T. Onimaru, T. Matsumura, M. Tsukagoshi, K. Kurauchi, H. Nitta, and T. Takabatake, *J. Phys. Soc. Jpn.* **93**, 034707 (2024).
- 55) R. Oishi, Y. Ohmagari, Y. Kusanose, Y. Yamane, K. Umeo, Y. Shimura, T. Onimaru, and T. Takabatake, *J. Phys. Soc. Jpn.* **89**, 104705 (2020).
- 56) R. Oishi, K. Umeo, Y. Shimura, T. Onimaru, A. M. Strydom, and T. Takabatake, *Phys. Rev. B* **104**, 104411 (2021).
- 57) R. Oishi, A. Miyake, M. Tokunaga, Y. Shimura, K. Umeo, T. Onimaru, and T. Takabatake, *J. Phys.: Conf. Ser.* **2164**, 012033 (2022).
- 58) R. K. Harris, E. D. Becker, S. M. Cabral de Menezes, R. Goodfellow, and P. Granger, *Pure Appl. Chem.* **73**, 1795 (2001).
- 59) N. J. Stone, *At. Data Nucl. Data Tables* **111–112**, 1 (2016).

- 60) G. C. Carter, L. H. Bonnet, and D. J. Kahan: Metallic Shifts in NMR (Pergamon Press, Oxford, 1977).
- 61) S. Kawasaki, T. Oka, A. Sorime, Y. Kogame, K. Uemoto, K. Matano, J. Guo, S. Cai, L. Sun, J. L. Sarrao, J. D. Thompson, and G.-q. Zheng, *Commun. Phys.* **3**, 148 (2020).
- 62) S. Doniach, *Physica B+C* **91**, 231 (1977).
- 63) H. v. Löhneysen, *J. Phys.: Cond. Matt.* **8**, 9689 (1996).
- 64) S. Kitagawa, S. Araki, T. C. Kobayashi, and Y. Ikeda, *J. Phys. Soc. Jpn.* **89**, 063702 (2020).
- 65) Y. Nakai, T. Iye, S. Kitagawa, K. Ishida, H. Ikeda, S. Kasahara, H. Shishido, T. Shibauchi, Y. Matsuda, and T. Terashima, *Phys. Rev. Lett.* **105**, 107003 (2010).
- 66) S. Kitagawa, T. Kawamura, K. Ishida, Y. Mizukami, S. Kasahara, T. Shibauchi, T. Terashima, and Y. Matsuda, *Phys. Rev. B* **100**, 060503(R) (2019).
- 67) K. Ishida, S. Matsuzaki, M. Manago, T. Hattori, S. Kitagawa, M. Hirata, T. Sasaki, and D. Aoki, *Phys. Rev. B* **104**, 144505 (2021).
- 68) J. Goryo, M. H. Fischer, and M. Sigrist, *Phys. Rev. B* **86**, 100507 (2012).
- 69) H. Watanabe, H. Seo, and S. Yunoki, *J. Phys. Soc. Jpn.* **86**, 033703 (2017).
- 70) R. Tazai, Y. Yamakawa, S. Onari, and H. Kontani, *Sci. Adv.* **8**, eabl4108 (2022).